hep-ph/9608418

TOP PHYSICS REVIEW AND OUTLOOK [a]

S. WILLENBROCK
Department of Physics, University of Illinois,
1110 West Green Street
Urbana, IL, 61801

I review the status of the top quark, and look forward to three topics relevant to future top-quark physics; spin correlation, single-top-quark production, and unification.

[a]Presented at the XXXI Rencontres de Moriond on Electroweak Interactions and Unified Theories, Les Arcs, Savoie, France, March 17-23, 1996.

1 Introduction

In this talk I review the status of the top quark, and then look forward to the future of top-quark physics. Top-quark physics is rich and varied, and I have chosen to present only a few specific topics which I find particularly interesting. The topics to be covered are

- Top-quark yields
- Top-quark mass and cross section
- Future top-quark physics
  - Spin correlation
  - Single-top-quark production
  - Top and unification

I end with a few concluding remarks.

2 Top-quark yields

Run I at the Fermilab Tevatron is now complete, and each experiment has accumulated an integrated luminosity of about 110 pb^{-1}. The peak luminosity achieved was about $\mathcal{L} = 2 \times 10^{31}/cm^2/s$, impressive for a machine that was designed for $\mathcal{L} = 10^{30}/cm^2/s$. The machine energy was 1.8 TeV.

Run II will begin in 1999, with a machine energy of 2 TeV. The increase in energy is made possible by cooling the magnets to a lower temperature, thereby allowing a higher field strength. This increases the top-quark production cross section by about 35%.

The most important change that will occur in Run II is a ten-fold increase in luminosity, to $\mathcal{L} = 2 \times 10^{32}/cm^2/s$. This will be achieved by two additions to the existing accelerator complex:

- Main Injector: The original Main Ring in the Tevatron collider tunnel is a bottleneck to higher luminosity. It will be replaced by the Main Injector, a 120 GeV synchrotron housed in a separate tunnel, now under construction. The Main Injector will enable the production of many more antiprotons, yielding a five-fold increase in luminosity.
- Recycler: The Recycler ring is an 8 GeV, low-field, permanent-magnet ring which will be installed in the Main Injector tunnel. The primary function of the Recycler is to allow more efficient accumulation of antiprotons. Its secondary role, from which it takes its

name, is to allow the reuse of antiprotons left over from the previous store. The Recycler will yield a two-fold increase in luminosity.

The improvements in the accelerator, along with a variety of detector upgrades, will result in a dramatic increase in the potential for top-quark physics in Run II. In $t\bar{t}$ events, the final state with the most kinematic information is $W + 4j$, where the W is detected via its leptonic decay. These events are fully reconstructable. To reduce backgrounds, it is best to demand at least one b tag. The number of such events is about $500/fb^{-1}$.[1)] Depending on the length of Run II, the integrated luminosity delivered to each detector will be between 1 and a few fb^{-1}. Thus there will be on the order of 1000 tagged, fully reconstructed top-quark events in Run II, to be compared with the approximately 25 $W + 4j$ single-tagged top events in Run I.

The CERN Large Hadron Collider (LHC) will provide another dramatic step forward in the potential for top-quark physics. The increase in machine energy results in an increase in the top-quark production cross section of about a factor of 100. The luminosity will range from $10^{33} - 10^{34}/cm^2/s$. Since b tagging is so important to top-quark physics, it may be advantageous to study the top quark at the lower end of the luminosity range, where b tagging is more effective. The increase in cross section, together with the increase in luminosity, result in about a million top-quark pairs per year at the LHC.[2)] The top-quark cross section and yield at the Tevatron and the LHC are summarized in Table 1.

Table 1: Schedule, machine parameters, top-quark cross section, and top-quark yield, for Run II at the Tevatron and for the LHC.

	Tevatron Run II	LHC
	1999	2004
$\sqrt{s}$	2 TeV	14 TeV
$\mathcal{L}$	$2 \times 10^{32}/cm^2/s$	$10^{33} - 10^{34}/cm^2/s$
$\sigma_{t\bar{t}}$	6.5 pb	750 pb
$W + 4j$ (b tag)	$500/yr$	$5 \times 10^5 - 10^6/yr$

There are also possibilities for top-quark physics beyond the Tevatron and the LHC. One proposal which is currently undergoing scrutiny is to increase the Tevatron luminosity yet further, to $10^{33}/cm^2/s$. The "Tev33", as it is called, might be useful for specialized top-quark studies, such as a measurement of the CKM matrix element V_{tb} (more on this later).

High-energy e^+e^- and $\mu^+\mu^-$ colliders provide a complementary tool to hadron colliders for top-quark physics. They have the unique capability of scanning the $t\bar{t}$ threshold region, but are

also useful above the threshold region. For lack of space, I will not be able to discuss top-quark physics at these colliders.

3 Top-quark mass and cross section

Preliminary values of the top-quark mass based on Run I data were presented at this conference by CDF and D0. Averaging these two measurements, assuming they are uncorrelated, yields a world-average top-quark mass of

$$m_t = 174.4 \pm 8.3 \text{ GeV} \quad (\text{CDF/D0}) \, . \tag{1}$$

It is anticipated that the error will be reduced to ± 4 GeV in Run II. The challenge to the Tev33 and the LHC is to go beyond this, perhaps to $\pm 1 - 2$ GeV.

The present measurement of the the W mass is

$$M_W = 80.330 \pm .150 \text{ GeV} \quad (\text{UA2/CDF/D0}) \, . \tag{2}$$

The error will be decreased in the near future by LEP II, and, somewhat later, by Run II at the Tevatron. A world-average error of less than ± 50 MeV is anticipated.

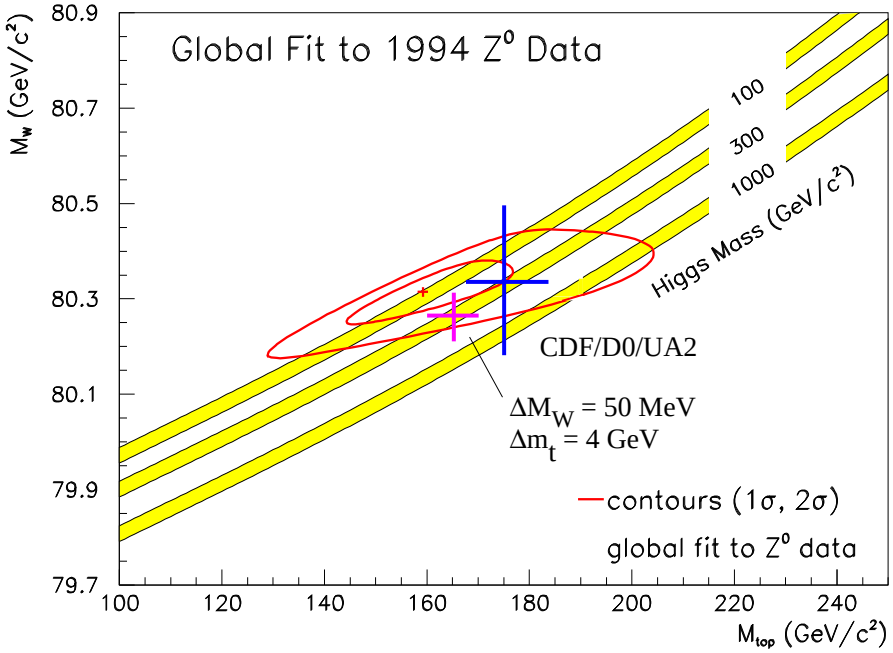

Figure 1: W mass vs. top-quark mass, with bands of constant Higgs mass. The contours are the one- and two-sigma regions from precision LEP and SLC data. The large cross is the direct measurement of M_W and m_t. The small cross, placed arbitrarily on the figure, is the anticipated uncertainty in M_W and m_t from LEP II and Run II at the Tevatron.

Figure 1 shows the well-known plot of M_W vs. m_t, with bands of constant Higgs mass. The contours show the one- and two-sigma fits to data from LEP and SLC, through 1994.[b] The large cross indicates the present direct measurements of M_W and m_t. The measurements are in good agreement with the precision electroweak data. The small cross indicates the errors expected from LEP II and Run II at the Tevatron, placed arbitrarily on the plot. These measurements have the potential of indicating a preferred range for the Higgs mass, or of indicating physics beyond the standard Higgs model.

The production of top-quark pairs occurs via the strong processes $q\bar{q}, gg \to t\bar{t}$. The top-quark cross section has been calculated at next-to-leading order in QCD.[3,4] The most recent update of this calculation is shown in Fig. 2, as a function of the top-quark mass.[5] The error band reflects the uncertainties in the uncalculated higher-order correction, in the parton distribution functions, and in α_s. The average of the CDF and D0 cross sections reported at this conference, for a top-quark mass of 175 GeV, is also shown in the figure. The agreement between theory and experiment is quite satisfactory.

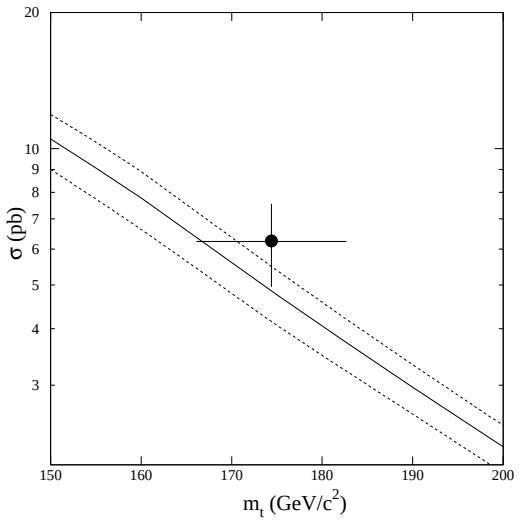

Figure 2: Theoretical cross section, with error band, for $t\bar{t}$ production at the Tevatron ($\sqrt{s} = 1.8$ TeV), versus the top-quark mass. The CDF/D0 average mass and cross section are indicated. Adapted from Ref. 5.

There are attempts to go beyond next-to-leading order in the theoretical calculation of the cross section.[5,6,7] Soft-gluon emission yields a correction proportional to $\alpha_s \ln^2 E/Q$, where E is the gluon energy and Q is the invariant mass of the $t\bar{t}$ pair. This leads to a large correction to the cross section, proportional to $\alpha_s \ln^2(s/4m_t^2 - 1)$, in the $t\bar{t}$ threshold region ($s \approx 4m_t^2$). Furthermore, these logarithmically-enhanced terms persist to all orders in perturbation theory, in the form $\alpha_s^n \ln^{2n} E/Q$. Fortunately, it is possible to sum these terms to all orders. However,

[b] The 1995 data is not yet available.

there is no universally-accepted technique for performing this summation at this time. Calculations lead to a correction, beyond next-to-leading order, of 1%,[5] 7%,[6] and 9%.[7] The most striking aspect of this is that theorists are concerned with a correction of order 10%. This is a great advance over the days, not so long ago, when QCD was considered successful if it agreed with data within 50%.

4 Future top-quark physics

4.1 Spin correlation

The top-quark lifetime is very short, $\Gamma_t^{-1} \approx (1.5 \text{ GeV})^{-1}$. This has the consequence that the top quark decays before the strong interaction has time to depolarize its spin.[8] To understand this clearly, let's recall the situation for the b quark, which is relatively long lived. A b quark hadronizes with a light antiquark into a $\overline{B}$ meson on a time scale Λ_{QCD}^{-1}. Its spin is then depolarized on a time scale $(\Lambda_{QCD}^2/m_b)^{-1}$, due to interactions of the light antiquark with the b-quark chromo-magnetic moment. The b quark decays, via the weak interaction, at a much later time. For the top quark, these last two stages are interchanged; the spin-depolarization time, $(\Lambda_{QCD}^2/m_t)^{-1} \approx (1.3 \text{ MeV})^{-1}$, is three orders of magnitude longer than the top-quark lifetime. Thus we expect the spin orientation of the top quark to be observable experimentally.

How does one go about testing this expectation? Fortunately, the weak decay of the top quark is sensitive to its spin orientation; the angular distribution of the top-quark's decay products acts as a spin analyzer. Unfortunately, top quarks produced via the strong processes $q\bar{q}, gg \to t\bar{t}$ are unpolarized, because the strong interaction is parity conserving. However, the spins of the t and $\bar{t}$ are correlated.[9,10,11,12] Thus if one observes this spin correlation experimentally, one has demonstrated that the top quark does indeed decay before the strong interaction has time to depolarize the top-quark's spin.

The differential cross section for $t\bar{t}$ production for different spin states is shown in Fig. 3, as a function of the $t\bar{t}$ invariant mass, at both the Tevatron and the LHC. The subscripts L and R denote the helicity. At the Tevatron, the t and $\bar{t}$ are mostly produced with the opposite helicity, while at the LHC they tend to have the same helicity. This difference is due to the fact that the dominant production process at the Tevatron is $q\bar{q} \to t\bar{t}$, while at the LHC it is $gg \to t\bar{t}$.

Since most of the total cross section comes from the threshold region, let's pause to reflect upon the origin of the spin correlation there. Near threshold, the t and $\bar{t}$ are produced in

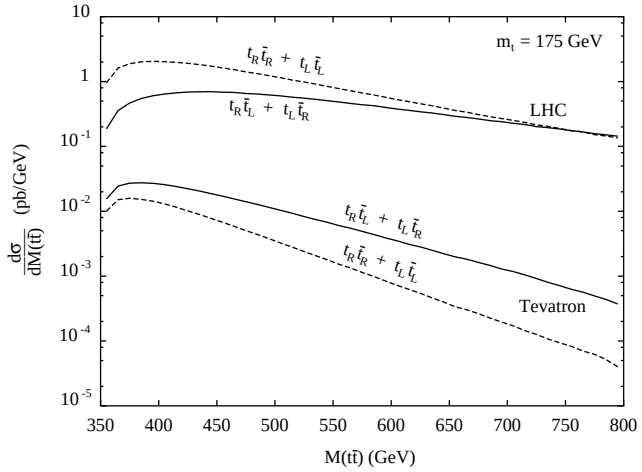

Figure 3: Differential cross section for top-quark pair production, vs. the $t\bar{t}$ invariant mass, for different helicity states, at the Tevatron and the LHC. From Ref. 11.

a state of zero orbital angular momentum. For $q\bar{q} \to t\bar{t}$, which is mediated by an s-channel gluon, the $t\bar{t}$ is an ${}^3S_1$ state. Two of these triplet states have the t and $\bar{t}$ spins aligned; since the quarks recede from each other back-to-back, this results in them having the opposite helicity two-thirds of the time. In the case of $gg \to t\bar{t}$, the $t\bar{t}$ is produced in a ${}^1S_0$ state, in which the spins are oppositely aligned, resulting in same-helicity $t\bar{t}$ pairs.

Although the spin correlation is large, its detection requires a significant amount of data. It should be observable, at the 3σ level, with 1000 $t\bar{t}$ events, as expected in Run II at the Tevatron. The observation is aided by analyzing the spins along the beam axis ("beamline basis"), rather than along the direction of motion of the quarks ("helicity basis").[10] At the LHC, the spin correlation will be easily observable, and may be a useful tool to study the weak decay properties of the top quark.

4.2 Single-top-quark production

There are two processes which produce a single top quark, rather than a $t\bar{t}$ pair: the W-gluon-fusion process,[13,14,15] depicted in Fig. 4(a), and $q\bar{q} \to t\bar{b}$,[16,17] shown in Fig. 4(b). Both involve the weak interaction, so they are suppressed relative to the strong production of $t\bar{t}$; however, this suppression is partially compensated by the presence of only one heavy particle in the final state. Both processes probe the charged-current weak interaction of the top quark. The single-top-quark production cross sections are proportional to the square of the Cabbibo-Kobayashi-Maskawa matrix element V_{tb}, which cannot be measured in top-quark decays since the top quark is so short-lived.

The cross sections for $t\bar{t}$, W-gluon fusion, and $q\bar{q} \to t\bar{b}$ are given in Table 2. The process

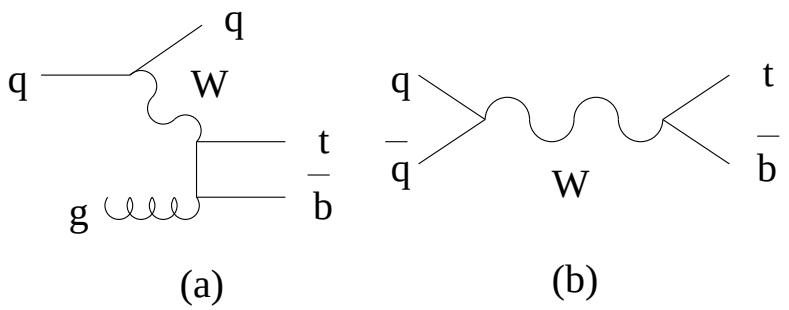

Figure 4: Single-top-quark production at hadron colliders: (a) W-gluon fusion; (b) quark-antiquark annihilation.

$q\bar{q} \to t\bar{b}$ is especially powerful as a measure of V_{tb} due to its similarity to the Drell-Yan process, $q\bar{q} \to \ell\bar{\nu}$. The Drell-Yan process can be used to help normalize the cross section, thereby reducing systematic uncertainties. The parton distribution functions are relatively well known, in contrast with the gluon distribution function involved in the W-gluon fusion process. At the LHC the process $q\bar{q} \to t\bar{b}$ is overwhelmed by backgrounds from $gg \to t\bar{t}$ and W-gluon fusion, since these processes are initiated by gluons. Thus the Tevatron provides a better environment for the measurement of this process.

Table 2: Approximate cross sections (pb) for top-quark production at the Tevatron ($\sqrt{s} = 2$ TeV) and the LHC.

	Tevatron	LHC
$t\bar{t}$	6.5	750
$Wg \to t\bar{b}$	2	200
$q\bar{q} \to t\bar{b}$	0.88	10

The cross section for $q\bar{q} \to t\bar{b}$ has been calculated at next-to-leading order in QCD.[18] The dominant sources of uncertainty are the parton distribution functions and the top-quark mass. A measurement of V_{tb} to an accuracy of 10% should be possible in Run II at the Tevatron, and perhaps to 4% with Tev33, assuming V_{tb} is close to unity.

4.3 Top and unification

The top quark is much more massive than the other known fermions, and this may provide a clue towards understanding nature at a deeper level. Nature has encouraged us to extrapolate the gauge couplings to high energy, where they are successfully unified (with the additional assumption of weak-scale supersymmetry) into a single SU(5) gauge coupling, g_U, at the GUT scale, $\sim 10^{16}$ GeV. The value of g_U is approximately $1/\sqrt{2}$, a number of order unity, as one would expect in a truly fundamental description of nature.

In supersymmetric models, fermion masses arise from their Yukawa coupling to one of the two Higgs fields, similar to the standard Higgs model (which has just one Higgs field). The Yukawa coupling of the top quark is of order unity at the weak scale. When extrapolated up to the GUT scale, it remains a number of order unity, which is encouraging. However, if the top quark were a bit heavier, its Yukawa coupling would blow up before reaching the GUT scale. Thus there is an upper bound of about 200 GeV on the top-quark mass in supersymmetric GUT models.[19] The fact that nature has chosen not to provide us with a quark heavier than this bound further encourages us to pursue supersymmetric grand unification.

The other fermions have very small Yukawa couplings, which is difficult to understand from a fundamental perspective. To a good approximation, they are zero in comparison with the top-quark's Yukawa coupling. An appealing explanation for this arises naturally in string theory. String theories are replete with discrete symmetries, and these symmetries make it difficult to have Yukawa couplings. The best that one can usually achieve, in the context of three generations of quarks and leptons, is one and only one nonvanishing Yukawa coupling, of order unity.[20,21] The hope is that the other Yukawa couplings, which are zero at leading order, arise from small perturbations to this scenario.

5 Conclusions

We are presently in the dawn of the top-physics era. The future promises a wealth of top physics at the Tevatron, LHC, and perhaps high-energy e^+e^- and $\mu^+\mu^-$ colliders. The large top-quark mass allows for accurate perturbative calculations of electroweak and strong top-quark processes. The experimental challenge is to match and surpass the accuracy of these calculations, in order to test the properties of the top quark with the greatest possible sensitivity. Since the top quark is by far the heaviest fermion, it would be a mistake to assume that its properties are simply those given by the standard model. Perhaps the top quark is exotic in some way, and will give us our first glimpse of physics beyond the standard model.

Acknowledgements

I am grateful for conversations with and assistance from G. Anderson, T. Liss, J. Lykken, R. Roser, and T. Stelzer. This work was supported in part by Department of Energy grant DE-FG02-91ER40677.

1. *Future Electroweak Physics at the Fermilab Tevatron: Report of the tev_2000 Study Group*, eds. D. Amidei and R. Brock, FERMILAB-Pub-96/082 (1996).
2. ATLAS Technical Proposal, CERN/LHCC/94-43.
3. P. Nason, S. Dawson, and R. K. Ellis, Nucl. Phys. **B303**, 607 (1988); **B327**, 49 (1989).
4. W. Beenakker, H.Kuijif, W. van Neeven, and J. Smith, Phys. Rev. D **40**, 54 (1989); W. Beenakker, W. van Neeven, R. Meng, G. Schuler, and J. Smith, Nucl. Phys. **B351**, 507 (1991).
5. S. Catani, M. Mangano, P. Nason, and L. Trentadue, hep-ph/9602208; hep-ph/9604351.
6. E. Laenen, J. Smith, and W. van Neerven, Nucl. Phys. **B369**, 543 (1992); Phys. Lett. **B321**, 254 (1994).
7. E. Berger and H. Contopanagos, Phys. Lett. **B361**, 115 (1995); hep-ph/9603326.
8. I. Bigi, Y. Dokshitzer, V. Khoze, J. Kühn, and P. Zerwas, Phys. Lett. **B181**, 157 (1986).
9. V. Barger, J. Ohnemus, and R. Phillips, Int. J. Mod. Phys. **A4**, 617 (1989).
10. G. Mahlon and S. Parke, Phys. Rev. D **53**, 4886 (1996).
11. T. Stelzer and S. Willenbrock, Phys. Lett. **B374**, 169 (1996).
12. A. Brandenburg, hep-ph/9603333.
13. S. Willenbrock and D. Dicus, Phys. Rev. D **34**, 155 (1986).
14. C.-P. Yuan, Phys. Rev. D **41**, 42 (1990); D. Carlson and C.-P. Yuan, Phys. Lett. **B306**, 386 (1993).
15. R. K. Ellis and S. Parke, Phys. Rev. D **46**, 3785 (1992).
16. S. Cortese and R. Petronzio, Phys. Lett. **B253**, 494 (1991).
17. T. Stelzer and S. Willenbrock, Phys. Lett. **B357**, 125 (1996).
18. M. Smith and S. Willenbrock, hep-ph/9604223.
19. J. Bagger, S. Dimopoulos, and E. Masso, Phys. Rev. Lett. **55**, 920 (1985).
20. A. Faraggi, Phys. Lett. **B278**, 131 (1992); Nucl. Phys. **B403**, 101 (1993).
21. S. Chaudhuri, G. Hockney, and J. Lykken, hep-th/9510241.